Chapter 5

Visualization of microbiological processes underlying stress relaxation in *Pseudomonas aeruginosa* biofilms

Brandon W. Peterson, Henk J. Busscher, Prashant K. Sharma, Henny C. van der Mei

(submitted)

ABSTRACT

Bacterial biofilms relieve themselves from external stresses through internal re-arrangement, which have been mathematically modeled in many studies, but never microscopically visualized for their underlying microbiological processes. Here, we apply a uniaxial 20% deformation to *Pseudomonas aeruginosa* biofilms and fixate deformed biofilms after allowing different periods of time for relaxation. Two *P. aeruginosa* mutant strains with different abilities to produce extracellular-polymeric-substances were involved in this study. The re-arrangement of extracellular-polymeric-substances and bacteria in deformed biofilms was visualized using confocal-laser-scanning-microscopy. Extracellular-polymeric-substances and bacteria showed distinct re-arrangements in time that differed between the mutant and its parent strain. This is the first visual confirmation of mathematical modeling of stress relaxation in biofilms, and points to a clear role of extracellular-polymeric-substances in their visco-elastic response.

INTRODUCTION

The protection offered by biofilms to inhabiting organisms against chemical and mechanical stresses is due in part to its unique matrix of extracellular-polymeric-substances (EPS) in which organisms embed themselves (5). Mechanical stresses lead to deformation and detachment of biofilm organisms and hence visco-elastic re-arrangement processes occur in a biofilm to relieve itself from these stresses (2). Environmental biofilms exposed to increased shear stress for instance, re-arrange into so-called streamers (15), i.e. extended portions of biofilm that can recoil when shear stresses return to normal levels. Also oral biofilms possess visco-elastic properties that allow them to better withstand mechanical stresses exerted by daily toothbrushing (1).

The re-arrangement processes occurring in biofilms under mechanical stress yield visco-elastic stress relaxation that can be analyzed using a Maxwell-model. Maxwell model analysis allows mathematical determination of characteristic relaxation time constants of the different relaxation processes occurring in a biofilm (14). Hitherto however, Maxwell-model analysis has only yielded mathematical descriptions of stress relaxation, but has not provided a more microbiologically-relevant description of internal re-arrangement processes in a biofilm (10,13,17). In general, three Maxwell elements suffice to mathematically describe stress relaxation of biofilms, and fastest Maxwell relaxation elements have been intuitively suggested to be due to the flow of water in mechanically stressed biofilms, as water has the smallest viscosity of all biofilm components (2,12). Since organisms themselves represent

the heaviest masses in a biofilm, their re-arrangement can be expected to coincide with the slowest Maxwell relaxation element. The array of stress relaxation elements with intermediate characteristic time constants ranging from 5 to 100 s, has been intuitively associated with re-arrangement of the EPS matrix (12). The aim of this study was to visualize the internal re-arrangement processes occurring in a mechanically deformed biofilm using confocal-laser-scanning-microscopy after propidium-iodide and calcofluor-white staining to visualize bacteria and EPS matrix, respectively. To this end, biofilms were grown with two *Pseudomonas aeruginosa* mutant strains with different abilities to produce EPS (6,16).

RESULTS AND DISCUSSION

Undeformed biofilms of EPS-producing *P. aeruginosa* SG81 demonstrate a fluorescence intensity distribution due to bacteria and EPS with maxima appearing at a depth of approximately 60 μm from the top of the biofilm (see Figure 1a). These maxima indicate elevated densities of bacteria and EPS at a certain distance from the top of the biofilm, without implying their absence at other depths made less visible through the Confocal laser scanning microscopy (CLSM) settings used (see Table 1) in order to visualize the elevated densities of EPS and bacteria. Immediately upon deformation (0 s relaxation), the centers of these intensity distributions appear at virtually the same depth as in undeformed biofilms (Figure 1b).

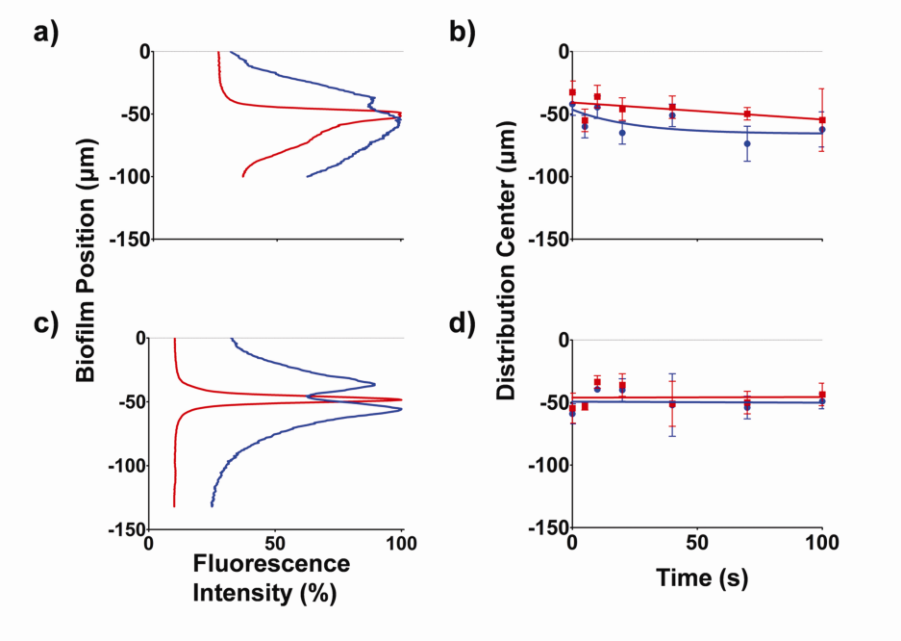

Figure 1. Distribution of EPS and bacteria in *P. aeruginosa* SG81 and *P. aeruginosa* SG81-R1 biofilms prior to mechanical deformation and after different stress relaxation times. Examples of the fluorescence intensity of propidium-iodine (RED) and calcofluor-white (BLUE) prior to deformation plotted as a percentage of the maximum intensity observed *versus* biofilm depth from its top (left panels), together with the positions of the centers of the intensity distributions as a function of the stress relaxation time (right panels). The positions of the distribution centers are presented as means of 12 images, taken equally divided over two separately grown biofilms, with error bars indicating the SD.
(a) and (b): *P. aeruginosa* SG81
(c) and (d): *P. aeruginosa* SG81-R1
(note that absolute intensities for EPS are very small for this strain).

However, since the thickness of the biofilm has been decreased due to the applied stress, there is no equilibrium and EPS and bacteria rapidly try to find new equilibrium positions in order to relieve the biofilm from the applied stress. Bacteria move away from the top of the biofilm to deeper layers in a linear fashion and even after 100 s of stress relaxation, have not found a new equilibrium position. EPS on the other hand, shows an exponential move toward deeper layers

and finds its new equilibrium position within 50 s. This demonstrates that re-arrangement of EPS in stress relaxation due to deformation proceeds on a faster time scale than re-arrangement of bacteria. This is in line with Maxwell-model analysis of stress relaxation processes in biofilms, showing that mathematically stress relaxation of biofilms can be described by three relaxation elements with different characteristic time constants of which the intermediate (5–100 s) one has been associated with flow of EPS and the slowest (>100 s) one with bacterial re-arrangement (7). The direct visualization of the microbiological processes underlying these two re-arrangements confirms the validity of the above intuitive association.

P. aeruginosa SG81-R1 produces hardly any EPS as compared with its parent strain *P. aeruginosa* SG81 (6,16), which is evidenced by the ratio of maximum fluorescence intensity of calcofluor-white over propidium-iodide, that is five-fold lower for *P. aeruginosa* SG81-R1 (0.11) than for *P. aeruginosa* SG81 (0.50). Both fluorescence distributions of bacteria and EPS for *P. aeruginosa* SG81-R1 fully coincide both before (Figure 1c) and after stress relaxation (Figure 1d), indicating that the small amount of EPS produced by this strain remains attached to the bacteria. The absence of a significant amount of EPS has a strong impact on the re-arrangement processes, as neither the centers of the intensity distributions for bacteria nor for EPS have moved to different depths within the 100 s time-span of the experiments. This suggests by comparison of the re-arrangement processes in *P. aeruginosa* SG81-R1 and *P. aeruginosa* SG81 biofilms, that EPS is required to stimulate bacterial movement in mechanically deformed biofilms. The mere presence of water as in *P. aeruginosa* SG81-R1 biofilms, may not be sufficient to

induce bacterial movement as it is much more loosely associated with the bacteria than EPS (4,5). Moreover, also the visco-elasticity of water is less than of EPS (3,8). Movement of EPS may thus be expected to drag bacteria along, with a certain time delay, as observed for EPS-producing *P. aeruginosa* SG81 but not for its mutant *P. aeruginosa* SG81-R1 within the time-scale of our experiments (Figures 1b and d).

This is the first study to visualize stress relaxation processes in *P. aeruginosa* biofilms due to re-arrangement of EPS and bacteria in deformed biofilms in a direct, microbiologically relevant way. The method utilized in this study is crude, to adapt for limitations of stain and laser penetration in CLSM (11) as well as for fixation capabilities of paraformaldehyde. Nevertheless, significant differences have been revealed between re-arrangement processes for EPS producing *P. aeruginosa* SG81 and its mutant strain *P. aeruginosa* SG81-R1. The re-arrangement processes visualized for *P. aeruginosa* SG81 proceed on a time-scale coinciding with mathematical analysis of stress relaxation processes in biofilms (7). Therewith this study provides a basis for more detailed structure-composition analysis of biofilms based on Maxwell-model analysis of stress relaxation.

MATERIALS AND METHODS

Two strains with different ability to produce EPS were selected for this study: *P. aeruginosa* SG81 and its mutant strain *P. aeruginosa* SG81-R1, largely deficient in EPS production (6,16). Bacteria were cultured in 10 ml nutrient broth (37°C, 17 h) and sonicated (10 W, 10 s, 0°C) to disrupt possible aggregates. Bacteria (1×10^8), suspended

in demineralized water, were deposited on a membrane filter (0.4 µm pore size, diameter 4.6 cm) under negative pressure and washed with 50 ml demineralized water. Subsequently, the filter was moved onto nutrient agar plates and incubated (37°C, 48 h) to grow a biofilm.

Biofilm-covered membranes were sectioned and transferred to glass slides. Deformation was imparted on the biofilms using a low-load-compression-tester (9). Briefly, a stainless steel plunger (diameter 0.25 cm) was lowered toward a sample stage and the position of the stage recorded. Next, the plunger was lowered toward the top of the biofilm till a touch load of 0.01 g and its position recorded again. The difference in plunger positions determined the biofilm thickness. Subsequently, biofilms were imparted a deformation of 20% in 1 s, and deformation was held constant for 0, 5, 10, 20, 40, 70, or 100 s. Deformed biofilms after different relaxation times were submerged in 3.7% (w/v) paraformaldehyde under continued deformation for 1500 s, after which the biofilm was stored overnight (17 h, 4°C) to fixate the state of the biofilms.

Paraformaldehyde was removed and biofilms were submerged in propidium-iodide (1.5 µl ml^{-1}, 18.3 mM), protected from light (20°C, 1 h). After propidium-iodide removal, biofilms were incubated in calcofluor-white (20 µl ml^{-1}, 3.8 mM) under identical conditions. After removal of calcofluor-white, biofilms were submerged in 50 ml sterile phosphate-buffered-saline (PBS, 5 mM K_2HPO_4, 5 mM KH_2PO_4, 150 mM NaCl pH 7.0), PBS was removed and biofilms were kept protected from light until imaging. Biofilms were imaged while submerged in PBS with a CLSM (see also Table 1) to visualize the

position of high density regions of bacteria and EPS after different relaxation times. Six regions of interest underneath the plunger area were chosen to quantify the fluorescence intensity due to each of the stains as a function of depth in the biofilm. All experiments were done on two separately grown biofilms for each strain.

Table 1. Confocal-laser-scanning-microscopy (Leica TCS-SP2, Leica Microsystems Heidelberg GmbH, Heidelberg, Germany) settings employed in this study.

Setting	**Propidium iodide (bacteria)**	**Calcofluor white (EPS)**
X-Y number of pixels	512	512
X-Y length of scan field	375 µm	375 µm
Pinhole	127.47 µm	204.57 µm
Zoom	1x	1x
Visible ATOF	(514 nm) 34.68%	(351 nm) 100%
Visible ATOF	(543 nm) 90.67%	(364 nm) 100%
Voltage	882.7 V	998.1 V
SP Mirror (left)	496 nm	409 nm
SP Mirror (right)	540 nm	551 nm
Objective	HCX APO L 40.0x0.80 W	HCX APO L 40.0x0.80 W
Numerical aperture	0.8	0.8

REFERENCES

1. **Busscher, H. J., D. Jager, G. Finger, N. Schaefer, and H. C. van der Mei.** 2010. Energy transfer, volumetric expansion, and removal of oral biofilms by non-contact brushing. Eur. J. Oral Sci. **118**:177-182.
2. **Cense, A. W., E. A. G. Peters, B. Gottenbos, F. P. T. Baaijens, A. M. Nuijs, and M. E. H. van Dongen.** 2006. Mechanical properties and failure of *Streptococcus mutans* biofilms, studied using a microindentation device. J. Microbiol. Methods **67**:463-472.
3. **Colvin, K. M., V. D. Gordon, K. Murakami, B. R. Borlee, D. J. Wozniak, G. C. L. Wong, and M. R. Parsek.** 2011. The Pel polysaccharide can serve as a structural and protective role in biofilm matrix of *Psuedomonas aeruginosa*. PLoS Pathog. **7**:e1001264.
4. **Flemming, H. C., T. R. Neu, and D. J. Wozniak.** 2007. The EPS matrix: the “house of biofilm cells”. J. Bacteriol. **189**:7945-7947.
5. **Flemming, H. C. and J. Wingender.** 2010. The biofilm matrix. Nat. Rev. Microbiol. **8**:623-633.
6. **Gomez-Suarez, C., J. Pasma, A. J. van der Borden, J. Wingender, H. C. Flemming, H. J. Busscher, and H. C. van der Mei.** 2002. Influence of extracellular polymeric substances on deposition and redeposition of *Pseudomonas aeruginosa* to surfaces. Microbiology **148**:1161-1169.
7. **He, Y., B. W. Peterson, M. A. Jongsma, Y. Ren, P. K. Sharma, H. J. Busscher, and H. C. van der Mei.** 2013. Stress relaxation analysis facilitates a quantitative approach towards antimicrobial penetration into biofilms. PLoS ONE **8**:e63750.
8. **Klapper, I., C. J. Rupp, R. Cargo, B. Purvedorj, and P. Stoodley.** 2002. Viscoelastic fluid description of bacterial biofilm material properties. Biotechnol. Bioeng. **80**:289-296.
9. **Korstgens, V., H. C. Flemming, J. Wingender, and W. Borchard.** 2001. Uniaxial compression measurement device for investigation of the mechanical stability of biofilms. J. Microbiol. Methods **46**:9-17.
10. **Lau, P. C., J. R. Dutcher, T. J. Beveridge, and J. S. Lam.** 2009. Absolute quantitation of bacterial biofilm adhesion and viscoelasticity by microbead force spectroscopy. Biophys. J. **96**:2935-2948.

11. **Mclean, J. S., O. N. Ona, and P. D. Majors.** 2008. Correlated biofilm imaging, transport and metabolism measurements via combined nuclear magnetic resonance and confocal microscopy. ISME. J. **2**:121-131.
12. **Peterson, B. W., H. J. Busscher, P. K. Sharma, and H. C. van der Mei.** 2012. Environmental and centrifugal factors influencing the visco-elastic properties of oral biofilms *in vitro*. Biofouling **28**:913-920.
13. **Picioreanu, C., M. C. van Loosdrecht, and J. J. Heijnen.** 2000. Effect of diffusive and convective substrate transport on biofilm structure formation: a two-dimensional modeling study. Biotechnol. Bioeng. **69**:504-515.
14. **Shaw, T., M. Winston, C. J. Rupp, I. Klapper, and P. Stoodley.** 2004. Commonality of elastic relaxation times in biofilms. Phys. Rev. Lett. **93**:098102.
15. **Stoodley, P., Z. Lewandowski, J. D. Boyle, and H. M. Lappin-Scott.** 1999. Structural deformation of bacterial biofilms caused by short-term fluctuations in fluid shear: an *in situ* investigation of biofilm rheology. Biotechnol. Bioeng. **65**:83-92.
16. **Strathmann, M., J. Wingender, and H. C. Flemming.** 2002. Application of fluorescently labelled lectins for the visualization and biochemical characterization of polysaccharides in biofilms of *Pseudomonas aeruginosa*. J. Microbiol. Methods **50**:237-248.
17. **Towler, B. W., A. Cunningham, P. Stoodley, and L. McKittrick.** 2007. A model of fluid-biofilm interaction using a Burger material law. Biotechnol. Bioeng. **96**:259-271.